J. Mol. Biol. (1989) **207**, 289–299

Ligand and Proton Exchange Dynamics in Recombinant Human Myoglobin Mutants

David G. Lambright, Sriram Balasubramanian and Steven G. Boxer†

Department of Chemistry
Stanford University, Stanford, CA 94305, U.S.A.

(Received 29 September 1988, and in revised form 13 December 1988)

Site-specific mutants of human myoglobin have been prepared in which lysine 45 is replaced by arginine (K45R) and aspartate 60 by glutamate (D60E), in order to examine the influence of these residues and their interaction on the dynamics of the protein. These proteins were studied by a variety of methods, including one and two-dimensional proton nuclear magnetic resonance spectroscopy, exchange kinetics for the distal and proximal histidine NH protons as a function of pH in the met cyano forms, flash photolysis of the CO forms, and ligand replacement kinetics.

The electronic absorption and proton nuclear magnetic resonance spectra of the CO forms of these proteins are virtually identical, indicating that the structure of the heme pocket is unaltered by these mutations. There are, however, substantial changes in the dynamics of both CO binding and proton exchange for the mutant K45R, whereas the mutant D60E exhibits behavior indistinguishable from the reference human myoglobin. K45R has a faster CO bimolecular recombination rate and slower CO off-rate relative to the reference. The kinetics for CO binding are independent of pH (6·5 to 10) as well as ionic strength (0 to 1 M-NaCl). The exchange rate for the distal histidine NH is substantially lower for K45R than the reference, whereas the proximal histidine NH exchange rate is unaltered. The exchange behavior of the human proteins is similar to that reported for a comparison of the exchange rates for myoglobins having lysine at position 45 with sperm whale myoglobin, which has arginine at this position. This indicates that the differences in exchange rates reflects largely the Lys → Arg substitution. The lack of a simple correlation for the CO kinetics with this substitution means that these are sensitive to other factors as well. Specific kinetic models, whereby substitution of arginine for lysine at position 45 can affect ligand binding dynamics, are outlined. These experiments demonstrate that a relatively conservative change of a surface residue can substantially perturb ligand and proton exchange dynamics in a manner that is not readily predicted from the static structures.

1. Introduction

The binding of ligands to myoglobin (Mb‡) has been the subject of extensive investigation and serves as a paradigm for understanding protein dynamics. X-ray structures for several ligated forms demonstrate that ligand access to the heme pocket is effectively blocked by the tight packing of protein residues (Kendrew *et al.*, 1960; Perutz & Matthews, 1966; Nobbs, 1966; Takano, 1977*a*,*b*). Nobbs (1966) suggested that structural fluctuations might create transient channels allowing penetration of ligands, and specific ligand trajectories were proposed by Case & Karplus (1979) on the basis of molecular dynamics simulations. A crystallographic study of sperm whale Mb, in which the heme pocket is forced open by ligation of a bulky phenyl group (Ringe *et al.*, 1984), reveals appreciable displacement of only three residues: arginine 45, histidine 64 and valine 68. It was argued that these residues might lie along a primary pathway for ligand access and binding. A high-resolution crystal structure has been reported for sperm whale Mb-CO, in which disorder at arginine 45 was modeled by two conformations, one of which does not block access to the heme pocket (Kuriyan *et al.*, 1986). This residue therefore appears to have some function related to ligand access.

† Author to whom all correspondence should be sent.

‡ Abbreviations used: Mb, myoglobin; n.m.r., nuclear magnetic resonance; fwhm, full width at half maximum; TSP, sodium 3-trimethyl silyl propionate; DSS, 4,4-dimethyl-4-sila pentane-1-sulfonate; p.p.m., parts per million.

0022–2836/89/090289–11 $03.00/0

It has been suggested that the interactions of arginine 45 with two carboxylate groups, those of aspartate 60 and the heme propionate of ring 4, serve to regulate ligand access (Ringe *et al.*, 1984; Lecomte & La Mar, 1985). In human Mb, the residue at position 45 is lysine. Although an X-ray structure is not available for this protein, one is available for seal Mb (Scouloudi & Baker, 1978), which also has lysine at this position. Interestingly, the nitrogen of its terminal amino group is within hydrogen-bonding distance of an oxygen atom of the heme propionate, but is too far from aspartate 60 for any appreciable interaction (Fig. 1). Although these studies suggest a role for arginine 45 in controlling ligand access, it remains to be demonstrated that substitutions at this site produce measurable effects on the kinetics or energetics of ligand binding.

One approach for probing the accessibility of the heme pocket relies on measuring the kinetics for the binding of diatomic ligands to deoxy Mb (Antonini & Brunori, 1971). The on-rate for CO association with deoxy Mb can be measured by monitoring the rate of recombination following flash photolysis of Mb-CO (Gibson, 1956; Antonini & Brunori, 1971; Austin *et al.*, 1975; Hasinoff, 1977, 1981; Alpert *et al.*, 1979; Duddell *et al.*, 1979, 1980; Friedman & Lyons, 1980; Beece *et al.*, 1980; Doster *et al.*, 1982; Henry *et al.*, 1983); the CO off-rate can be obtained by following the kinetics for the replacement of CO with NO (Gibson & Roughton, 1957; Antonini & Brunori, 1971; Wittenberg *et al.*, 1986).

An alternative approach involves measurement of proton exchange kinetics, which conveys information regarding the solvent accessibility of exchange sites (Hvidt & Nielsen, 1966; Woodward & Hilton, 1979; Woodward *et al.*, 1982; Roder *et al.*, 1985). This approach, in principle, provides the opportunity to explore heme pocket accessibility when a ligand is bound. Saturation transfer can be used to measure the exchange rates for protons having spin lattice relaxation and exchange rates of the same order of magnitude (Pitner *et al.*, 1974; Waelder *et al.*, 1975; Waelder & Redfield, 1977; Krishna *et al.*, 1979). In a solution study of the met cyano forms of horse, dog and sperm whale Mbs (Lecomte & La Mar, 1985), similar exchange rates were observed for the ring NH proton of the distal histidine in the horse and dog proteins, both of which have lysine at position 45, while the same proton in sperm whale Mb, which has arginine at this position, exhibited markedly slower exchange at high pH. The on-rates for CO recombination in these proteins, however, do not correlate with the substitution of arginine for lysine (Goss *et al.*, 1982).

An obvious shortcoming of comparisons among proteins from different species is the large number of amino acid substitutions that occur in addition

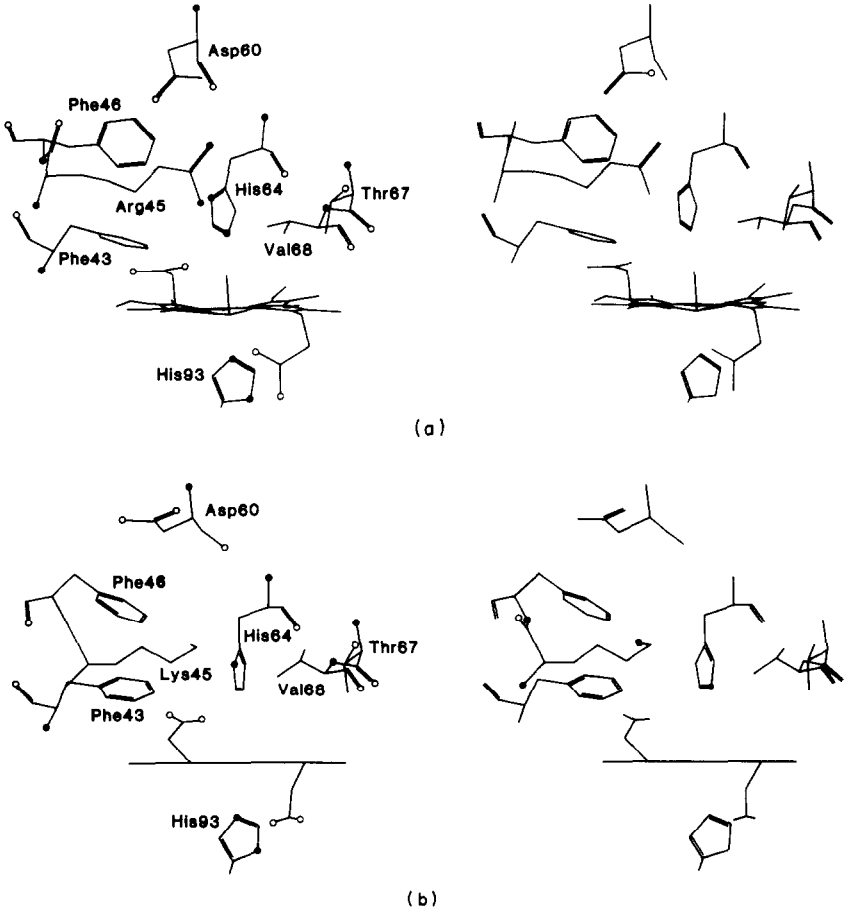

Figure 1. Stereo views of selected residues in the distal region of (a) sperm whale met Mb (Takano, 1977*b*), where residue 45 is arginine and (b) seal met Mb (Scouloudi & Baker, 1978), were residue 45 is lysine.

to that at the position of interest. This situation has changed markedly with the advent of site-specific mutagenesis (Zoller & Smith, 1983), and the availability of clones and expression systems for Mb (Varadarajan *et al.*, 1985; Springer & Sligar, 1987). Thus, it is now possible to focus on the consequences of changes in individual residues. We have prepared two mutants of human Mb to examine the roles of residues 45 and 60 in ligand binding: one in which lysine 45 is replaced with arginine (K45R), and a second in which aspartate 60 is replaced with glutamate (D60E) in order to perturb the interaction between residues 45 and 60. Table 1 summarizes these changes and indicates the amino acid at position 45 for all of the proteins that will be discussed. We report here a detailed characterization of the effects of these mutations on both on and off-rates for CO binding, as well as exchange kinetics for two protons in the heme pocket of the met cyano forms.

2. Materials and Methods

(a) *Protein preparation*

Site-specific mutants of human Mb were prepared according to the method of Kunkel (1985). The DNA for each mutant was sequenced in the region of the mutation to ensure that no other changes had occurred. Proteins were expressed in AR68 under geopen selection as described earlier (Varadarajan *et al.*, 1985). The protocol for purification has been modified slightly and is reported elsewhere (Varadarajan *et al.*, 1988). Cysteine 110 has been replaced with alanine in human Mb as well as the K45R and D60E mutants. This substitution simplifies purification of the proteins, since cysteine is susceptible to oxidation. Alanine does not alter any of the properties that we have studied to date (Varadarajan, 1988), and we therefore use the mutant C110A as a reference for the other mutants and designate it as the wild-type for purposes of discussion (see Table 1).

Protein purity was checked by isoelectric focusing at 4 °C. Wild-type, K45R and D60E were observed to have the same isoelectric point (data not shown). All 3 proteins are stable to tryptic digestion, as this is an essential feature of their preparation (Varadarajan *et al.*, 1985). Further, the electronic absorption spectra of the 3 proteins are virtually identical in different oxidation and liganded forms, as are the chemical shifts of all protons in the CO forms that have been assigned (more than 60 to date; unpublished results) in the 2-dimensional n.m.r. spectra. Thus, there is no evidence for differences between the solution structures of any of these proteins and that for sperm whale Mb (Antonini & Brunori, 1971; Mabbutt & Wright, 1985; Dalvit & Wright, 1987).

Table 1

Summary of myoglobins discussed in the text

Myoglobin	Mutation†	Residue at position 45	No. of amino acid differences from human wild-type
Human wild-type		Lysine	—
Human K45R	Lys45 → Arg	Arginine	1
Human D60E	Asp60 → Glu	Lysine	1
Sperm whale		Arginine	25
Horse		Lysine	19
Dog		Lysine	23
Seal		Lysine	24

† Wild-type and mutant human Mbs all have the substitution Cys110 → Ala (see Materials and Methods).

(b) *Measurement of* k_{on} *by flash photolysis*

Samples for photolysis were prepared immediately prior to use. Concentrated solutions of the met aquo forms of the proteins were diluted to an absorbance at 409 nm of approx. 1·0 with a buffer consisting of 50 mM-potassium phosphate and 50 mM-potassium borate. The solutions were equilibrated with CO at 1 atm (101,325 Pa) and then reduced by addition of sodium dithionite to a final concentration of 10 mM. Protein concentrations were estimated from the absorbance at 423 nm using an extinction coefficient of 187,000 M^{-1} cm^{-1} (Antonini & Brunori, 1971). All experiments were conducted at ambient temperature (22 °C).

Samples were photolyzed using 10 ns (fwhm) pulses from the 532 nm doubled output of a Q-switched Nd : YAG laser operating with a repetition rate of 10 Hz. The power was attenuated using neutral density filters to an energy density of 1 mJ/cm^2 at the sample resulting in 10% photolysis. The bimolecular recombination event was followed by monitoring the transient absorbance changes at 434 nm. Under the conditions of our experiment, the observed rate of recombination is pseudo 1st order in the concentration of deoxy Mb, and pseudo 1st-order rate constants were obtained from a non-linear least-squares fit of the data to a single exponential. These were converted into 2nd-order rate constants using published constants for the solubility of CO in aqueous solutions (Seidell, 1940; Wiesenburg & Guinasso, 1979). Approximate relative geminate recombination yields were obtained by measuring the initial ΔA_{434} following excitation of samples with identical absorbance at 532 nm. Sperm whale Mb, whose geminate recombination yield has been determined accurately (Henry *et al.*, 1983), was used as a standard for comparison.

(c) *Measurement of* k_{off} *by replacement of CO with NO*

Concentrated stock solutions of Mb-CO were prepared by stirring metMb in 50 mM-phosphate buffer (pH 6·6) under CO for 15 min, adding 2 equivalents of freshly prepared sodium dithionite solution, and stirring under CO for a further 30 min. NO-saturated buffer was prepared by bubbling NO gas through a deoxygenated solution of 50 mM-phosphate buffer (pH 6·6) for 15 min. A small quantity of the Mb-CO stock was then injected and the reaction followed by monitoring the absorbance change at 424 nm, corresponding to the maximum of the difference spectrum between Mb-CO and Mb-NO. Under these conditions (total [CO] = 6 μM, total [NO] = 2 mM) the reaction is 1st order and the decay was fit to a single exponential using a non-linear least-squares fitting program. Highly reproducible results were obtained with different preparations of the proteins.

(d) *Proton nuclear magnetic resonance spectroscopy*

Samples of the metcyano forms were prepared from 0·5 mM solutions of the purified proteins in 10% ^2H_2O/90% H_2O. NaCN was added to a concentration of 20 mM and the pH adjusted to 5·5 with HCl. The

solutions were then made 200 mM in NaCl, filtered through 0·45 μm filters, and the protein concentrated to between 5 and 6 mM. All subsequent adjustments to the pH were made by addition of 1 M-NaOH in 10% ^2H_2O. The pH was measured with an Ingold microcombination electrode and was not corrected for isotope effects. The temperature was maintained at 36°C for all experiments.

^1H n.m.r data were recorded at 500 MHz on a GE GN500 spectrometer using a 16-bit ADC. Suppression of the water peak was achieved using the uniform excitation pulse sequence 1-τ-3-τ-$\bar{3}$-τ-$\bar{1}$ (Wang & Pardi, 1987). Chemical shifts are referenced to TSP indirectly using dioxane as an internal standard. The n.m.r. data were processed using the FTNMR software written by Dennis Hare. Peak areas and linewidths were calculated from a non-linear least-squares fit of the spectral regions of interest to a sum of Lorentzians.

Proton exchange rates were calculated from the measured saturation factors and selective T_1 values as described by Lecomte & La Mar (1985). Saturation transfer experiments consisted of 2 interleaved spectra, one in which the water line was saturated with a 1 s decoupler pulse, and a reference spectrum in which the decoupler was placed off resonance. Saturation factors were calculated from the ratio of the area for a peak in the water-saturated spectrum (I) and that for the same peak in the reference spectrum (I_0). Selective T_1 values were obtained from saturation recovery experiments in which the peak of interest was selectively saturated with a pulse from the decoupler while the H_2O line was saturated at all times except during acquisition. At those pH values where measurable saturation transfer was observed, selective relaxation rates, ρ, were estimated from the effective relaxation rates, ρ', using the relation $\rho = \rho' F$, where F is the measured saturation factor given by $F = I/I_0$. Selective T_1 values were obtained from a 3-parameter non-linear least-squares fit (Levy & Peat, 1975).

3. Results

(a) *Measurements of* k_{on}

Representative decay kinetics for CO recombination after photolysis are shown in Figure 2 for sperm whale Mb and the three human proteins. Photolysis experiments were repeated using samples of the same proteins from several different preparations. It was found that the largest source of random error was associated with the equilibration of the samples with CO and not with the preparation of the proteins. Further protein purification by anion-exchange chromatography did not result in detectable differences for any of the experimental values. The second-order rate constants (k_{on}) are given in Table 2. The errors represent the standard deviations of at least four independent measurements.

We obtain a value of $0{\cdot}733(\pm 0{\cdot}04) \times 10^6$ M^{-1} s^{-1} for k_{on} at pH 6·5 for sperm whale Mb, in agreement with the value of $0{\cdot}72(\pm 0{\cdot}01) \times 10^6$ M^{-1} s^{-1} at pH 7·0 reported by Henry *et al.* (1983). The recombination rate for wild-type human Mb is faster by a factor of 1·35 ($k_{on} = 0{\cdot}986(\pm 0{\cdot}05) \times 10^6$ M^{-1} s^{-1}). Goss *et al.* (1982) reported CO association rates for Mbs from a number of different species including human and sperm whale. Their values for k_{on} differ from ours and those of Henry *et al.* (1983) for sperm whale Mb

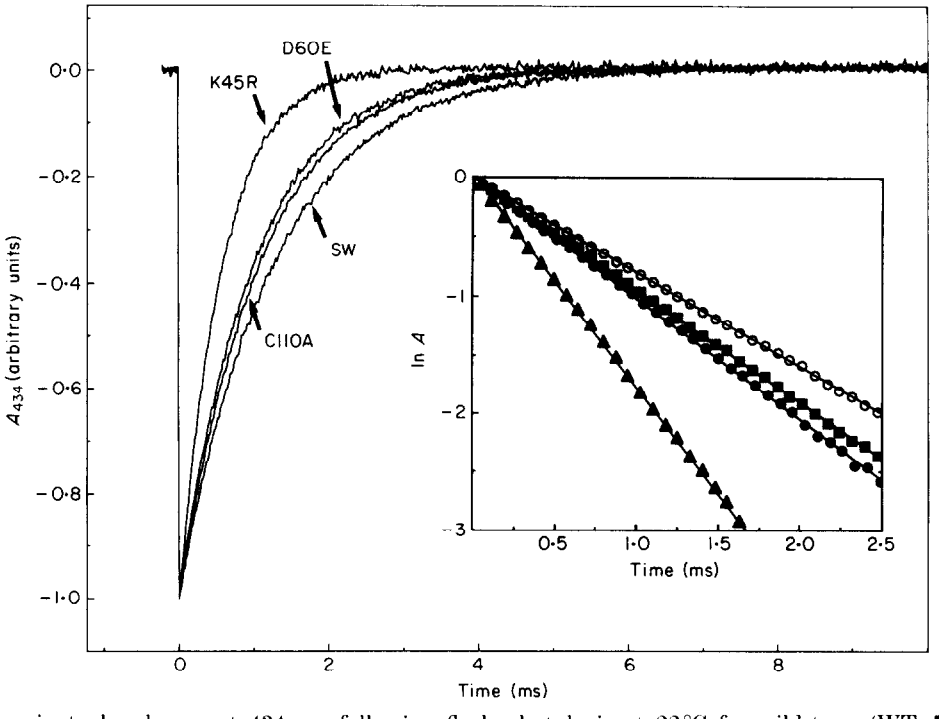

Figure 2. Transient absorbance at 434 nm following flash photolysis at 22°C for wild-type (WT, ■), K45R (▲), D60E (●) human Mb-CO and sperm whale (SW, ○) Mb-CO. The raw data have been normalized to unit absorbance at zero time in order to facilitate comparison. Inset: semi-log plot of the same data. The lines are obtained from linear least-squares fits to the data.

Table 2
Kinetic constants for CO binding

Myoglobin	$k_{on} \times 10^{-6}$ ($M^{-1}\ s^{-1}$)	$k_{off} \times 10^{2}$ (s^{-1})	$k_{on}/k_{off} \times 10^{-7}$ (M^{-1})
Human wild-type	0·986±0·05	3·61±0·20	2·73±0·21
K45R	1·80±0·12	2·50±0·11	7·23±0·58
D60E	1·07±0·06	3·56±0·16	3·09±0·22
Sperm whale	0·733±0·04	2·90±0·20	2·36±0·21

by a factor of 1·5; however, the relative rates measured by Goss and co-workers for human and sperm whale Mb are the same as we observe. Replacement of lysine 45 in human Mb with arginine produces a surprising result; k_{on} becomes faster by a factor of 1·8 ($k_{on} = 1{\cdot}80(\pm 0{\cdot}12)$ $M^{-1}\ s^{-1}$), rather than slower as initially expected on the basis of the slower on-rate for the sperm whale protein. This is especially significant, since it represents the first case in which the effects of this substitution have been isolated. The D60E mutation, on the other hand, produces no significant change in the on-rate ($k_{on} = 1{\cdot}07(\pm 0{\cdot}06) \times 10^{6}$ $M^{-1}\ s^{-1}$) compared with wild-type. The rates show no dependence (data not shown) on either pH (6·5 to 10) or ionic strength (0 to 1·0 M-NaCl) after correction for the solubility of CO in NaCl solutions (Seidell, 1940; Wiesenburg & Guinasso, 1979). For most heme proteins, ϕ_{gem} for CO recombination is very low (<0·1: Henry *et al.*, 1983; Gibson *et al.*, 1986; Olson *et al.*, 1987). For sperm whale Mb, Henry *et al.* (1983) observe $\phi_{gem} = 0{\cdot}04$. Based on this value, we find that ϕ_{gem} for wild-type is less than a factor of 3 larger than sperm whale Mb, while ϕ_{gem} for K45R is less than a factor of 1·5 larger than wild-type.

(b) *Measurement of* k_{off}

The time-courses for CO replacement by NO for sperm whale Mb and the three human proteins are presented in Figure 3, and the values of k_{off} are summarized in Table 2. The standard deviations in the values of k_{off} are based on at least three experiments for each protein. Apparent binding constants, $K_{app} = k_{on}/k_{off}$, are given in Table 2. Human Mb and the mutant D60E have the highest off-rates, and these rates are the same within experimental error. Interestingly, the mutant K45R has an off-rate that is smaller than the wild-type by a factor of 0·7. Note that sperm whale Mb also has a smaller off-rate than wild-type human Mb, though still larger than the mutant K45R. Thus, K45R has the highest apparent binding constant, $7{\cdot}2 \times 10^{7}$ M^{-1}, a result of both a higher on-rate and a lower off-rate. The D60E mutant has k_{off} and binding constant values equal to the wild-type within the experimental error.

(c) *Proton nuclear magnetic resonance spectroscopy*

Assignments for many of the hyperfine shifted peaks in the downfield region of the ^{1}H n.m.r. spectrum of sperm whale met Mb-CN have been reported (Sheard *et al.*, 1970; Mayer *et al.*, 1974;

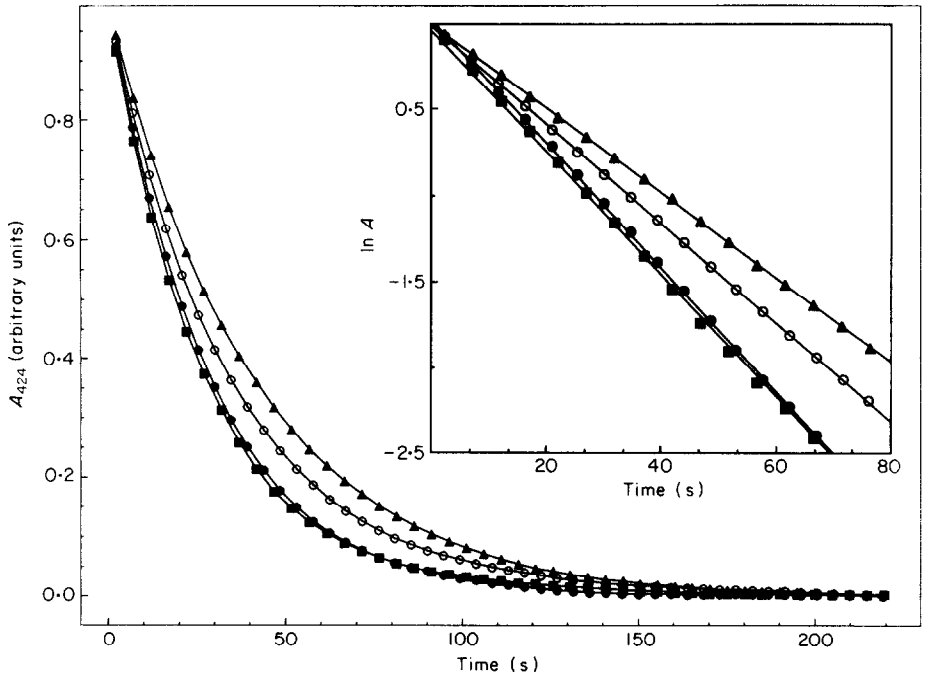

Figure 3. First-order kinetics at 22 °C for replacement of CO with NO for wild-type (WT, ■), K45R (▲), D60E (●) human Mb-CO and sperm whale (SW, ○) Mb-CO. The raw data have been normalized to unit absorbance at zero time in order to facilitate comparison. Inset: semi-log plot of the same data. The lines are obtained from linear least-squares fits to the data.

Cutnell *et al.*, 1981; La Mar & Krishnamoorthi, 1983). These assignments have been applied to the corresponding peaks for the met Mb-CN forms of horse and dog Mbs (Lecomte & La Mar, 1985). Figure 4 displays a portion of the downfield region of the 500 MHz ^{1}H n.m.r. spectra of the met Mb-CN forms of the human proteins in 10% ^2H_2O/90% H_2O at pH 9·25 and 36°C. The features of the wild-type spectrum are remarkably conserved in the spectra of the two site-specific mutants, both in the downfield and the upfield regions (data not shown). These spectra also exhibit a high degree of similarity to those of the sperm whale, horse and dog met Mb-CN (Lecomte & La Mar, 1985). In view of this, and the fact that the amino acid residues lining the heme pocket are identical in all these species, it is possible to extend several of the assignments to the human proteins as well. These assignments in the human proteins were confirmed by observation of equivalent NOE connectivities in the human proteins (data not shown) and in sperm whale Mb (Emerson *et al.*, 1988). The chemical shifts for a number of these resonances are given in Table 3. Note, in particular, the exchangeable resonances at ~22·0 and ~20·7 p.p.m., which can be identified with imidazole NH protons of the distal (His64) and proximal (His93) histidine residues, respectively.

Saturation factors for the imidazole NH protons of the distal and proximal histidine residues are shown in Figure 5 as a function of pH for the wild-type protein and the two mutants. The saturation behavior of the proximal histidine NH is virtually identical, within experimental error, for the three proteins; saturation factors are observed to be unity below pH 8 and fall off steadily with increasing pH in the range from 8 to 10·5. The distal histidine NH of K45R, on the other hand, exhibits markedly different saturation behavior compared with wild-type. The degree of saturation transfer is reduced over the entire pH range, particularly above pH 8. The saturation behavior of the D60E distal histidine NH quite closely resembles that of wild-type, although it exhibits slightly reduced saturation transfer, which is again more pronounced at

Table 3

^{1}H n.m.r. chemical shifts for selected resonances of various myoglobins in the met cyano form, pH 9·25, 36°C (in p.p.m. from TSP)

	Myoglobin			
Resonance	Wild-type	Human K45R	D60E	Sperm whale†
Heme 1-CH_3	17·57	17·57	17·57	17·67
Heme 5-CH_3	26·01	26·04	26·04	25·58
Heme 8-CH_3	12·58	12·47	12·58	12·50
His64 NH	22·05	22·10	22·21	22·33
His93 NH	20·67	20·67	20·70	20·35
Ile67 CG	−3·35	−3·33	−3·37	−3.00
Ile97 CD	−4·00	−3·92	−4·04	−3·33

† From Lecomte & La Mar (1985); shifts are in p.p.m. from DSS at pH 8·6 and 40°C.

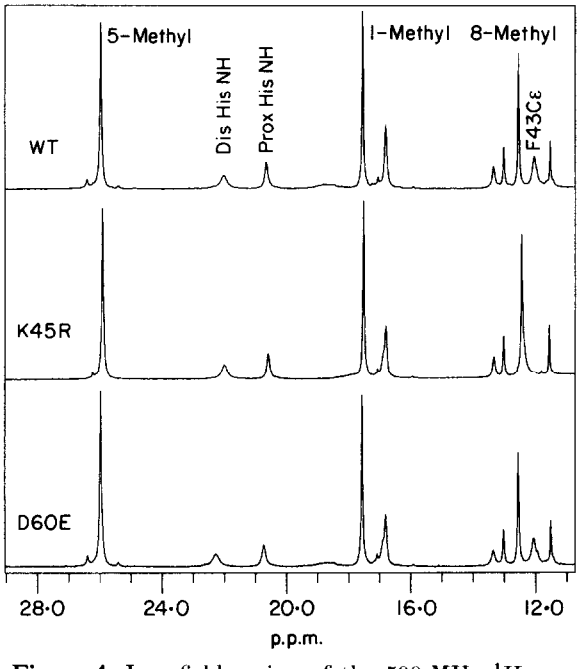

Figure 4. Low-field region of the 500 MHz ^{1}H n.m.r. spectra of the met cyano form of wild-type (WT), K45R, and D60E human Mbs. Samples contain 4 to 7 mM-protein and 200 mM-NaCl in 10% ^2H_2O/90%H_2O, pH 9·25, 36°C.

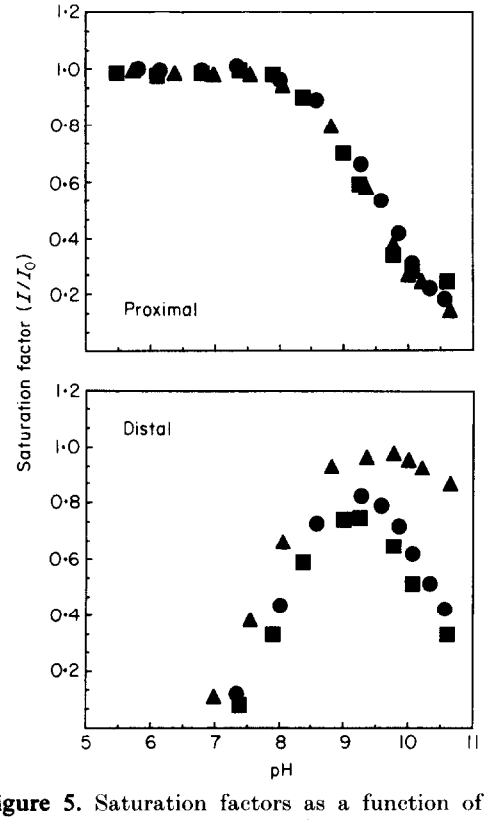

Figure 5. Saturation factors as a function of pH at 36°C for imidazole NH protons of the proximal and distal histidine residues in the met cyano forms of wild-type (■), K45R (▲), and D60E (●) human Mbs.

higher pH. Selective T_1 values were determined at low pH for the proximal histidine NH groups and at a pH of approximately 9·25 for the distal histidine NH groups. After correction for saturation transfer, variations in measured T_1 values between the various human proteins fall within the 5% statistical error estimated for the selective T_1 values on the basis of reproducibility (Table 4).

Exchange rates calculated from saturation factors and selective T_1 values are plotted as a function for pH in Figure 6. Clearly, the important features of the saturation behavior are preserved in the exchange rates. The proximal histidine NH exchange rates are essentially identical for the three proteins and increase steadily with pH. This is consistent with the assignment of these protons to the imidazole groups of the proximal histidine, since the strong Fe–N (H93) bond is expected to effectively eliminate acid-catalyzed exchange (Cutnell *et al.*, 1981). The distal histidine NH exchange rates for wild-type and D60E are characterized by a minimum at approximately pH 9·2, with D60E being only slightly slower, most noticeably at higher pH. In contrast, the exchange minimum for K45R is shifted to higher pH. As a consequence of the exceptionally rapid relaxation of the distal histidine NH, it is difficult to obtain reliable values for exchange rates less than about 10 s^{-1}, where the magnitude of the statistical error becomes comparable to the exchange rate. Likewise, it is difficult to determine the pH minimum precisely. However, it is noted that maximum values of the saturation factors as well as minimum values of the linewidths for the distal histidine NH resonance in K45R are attained at pH 9·8. Thus, the pH minimum for K45R is increased by about 0·6 pH unit relative to wild-type, an estimate that is consistent with the larger differences observed in the base-catalyzed as compared to the acid-catalyzed exchange rates.

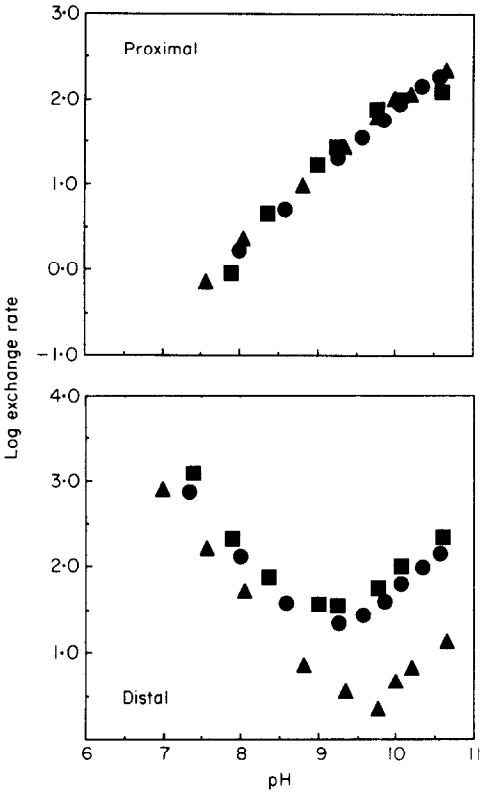

Figure 6. Exchange rates as a function of pH at 36°C for imidazole NH protons of the proximal and distal histidine residues in the met cyano forms of wild-type (■), K45R (▲), and D60E (●) human Mbs.

4. Discussion

Replacement of lysine 45 with arginine (K45R) in human Mb allows, for the first time, the effects of this substitution to be examined in the absence of other changes. Although this mutation is fairly conservative, significant changes are observed in both on and off-rates of ligand binding, demonstrating unequivocally that the nature of the residue at position 45 influences the access of ligands to the heme pocket. It is surprising that K45R has a faster on-rate than wild-type, particularly since the on-rate for sperm whale Mb, which also has arginine at position 45, is slower than wild-type human Mb. Evidently, other amino acid substitutions contribute to the overall difference in ligand on-rates between human and sperm whale Mb, illustrating the dangers of making comparisons among species with many primary sequence differences. In contrast to the 1·8-fold increase in k_{on} observed for CO recombination to K45R, k_{off} is slower by a factor of 1·45 relative to wild-type, implying that an increase has occurred in the apparent equilibrium binding constant (k_{on}/k_{off}) for CO. Interestingly, substitution of glutamate for aspartate at position 60 in D60E has little effect on any measure of ligand or proton exchange dynamics. Computer graphics modeling using both the seal and sperm whale Mb structures suggests that simultaneous interaction of lysine 45 with both the 6-propionate of the heme ring and the residue at position 60 would be possible for D60E, but not for wild-type, unless it was accompanied by large structural rearrangements. Since we have no

Table 4

Selective T_1 *values*† *for proximal and distal histidine NH resonances at 36°C*

	Proximal		Distal	
Protein	pH	T_1 (ms)	pH	T_1 (ms)
Wild-type	5·5	25·3	9·25	9·3
K45R	5·7	26·0	9·35	9·9
D60E	5·1	24·5	9·25	9·7
SWMB‡	4·7	25·0	9·2	8·9

† Calculated from T_1 (selective) = T_1 (measured)/F, as described in the text.

‡ From Lecomte & La Mar (1985). Selective T_1 values for sperm whale Mb (SWMb) are at 40°C.

evidence for major structural differences among any of these proteins, the absence of effects when glutamate is substituted for aspartate, as well as the absence of ionic strength effects, suggest that even if salt-bridge interactions exist between lysine 45 and the residue at position 60, they do not contribute significantly to the observed kinetics. In the following, we focus on possible mechanisms to explain the large effects resulting from substitution of arginine for lysine at position 45.

(a) *Proton n.m.r. and exchange kinetics*

La Mar and co-workers have demonstrated unequivocally that hyperfine-shifted resonances in the ^{1}H n.m.r. spectra of low-spin ferric heme proteins are exquisitely sensitive indicators of the heme electronic state as well as the local structure of the heme pocket (La Mar, 1979; La Mar *et al.*, 1980). The chemical shifts of protons attached to the heme ring arise largely from a contact mechanism and therefore reflect the distribution of unpaired spin density. The shifts of the 1, 5 and 8-methyl groups are nearly identical for each of the three human proteins (as well as sperm whale Mb) in the met cyano form, demonstrating that the ground state electronic structure of the heme ring is unperturbed by the substitutions we have made at positions 45 and 60. Likewise, only small (<0·3 p.p.m.) differences are observed for hyperfine shifted resonances arising from protein side-chain protons, indicating that these side-chains are also unperturbed in the met cyano form.

The consequences of the Lys → Arg substitution at position 45 with regard to the equilibrium solution structure of the heme pocket can be further explored by comparison of the 500 MHz ^{1}H n.m.r. spectrum of the CO forms of wild-type and K45R. More than 60 resonances arising from 25 residues mostly in or near the heme pocket have been assigned in the human proteins by two-dimensional methods. Despite the fact that many of these resonances exhibit a large distance and orientation-dependent contribution to the chemical shift from the large ring current of the heme macrocycle, no differences in chemical shift larger than 0·1 p.p.m. are observed. We therefore conclude that the solution structure of the heme pocket is conserved in these proteins and, in particular, that the ensemble averaged conformations of the heme pocket residues histidine 64 (distal His) and phenylalanine 43, which potentially lie within van der Waals' contact of residue 45, have been minimally perturbed by the Lys → Arg substitution.

In a detailed comparison of horse, dog, and sperm whale met cyano Mbs by n.m.r., Lecomte & La Mar (1985) have observed a substantially slower exchange rate above pH 9 for the distal histidine NH resonance in the sperm whale protein. They attributed this difference to the substitution of arginine for lysine at position 45 in these species. Following their work, we have measured exchange rates for the same protons in the wild-type and two mutants of human Mb. Wild-type human Mb exhibits exchange behavior that parallels that for horse and dog Mbs, while the K45R mutant resembles the sperm whale protein in that the exchange rates at high pH are substantially reduced compared with the other proteins. Thus, the substitution of arginine for lysine largely accounts for the slower exchange rate of the distal histidine NH resonance in sperm whale Mb. K45R appears to differ from sperm whale Mb in that the former exhibits a minimum in the distal histidine NH exchange rate at pH 9·8, whereas Lecomte & La Mar did not observe such a minimum for sperm whale Mb even up to pH 10·5, the highest pH in their experiments.

Hydrogen exchange rates in proteins have commonly been interpreted in terms of a two-state model characterized by three kinetic constants (Hvidt & Nielsen, 1966; Woodward & Hilton, 1979; Woodward *et al.*, 1982; Roder *et al.*, 1985):

$$\mathrm{N} \underset{k_{-1}}{\overset{k_1}{\rightleftharpoons}} \mathrm{I} \xrightarrow{k_2} \text{exchange}, \qquad (1)$$

where N represents a conformational state in which exchange at the site of interest is immeasurably slow, and I is a state in which exchange occurs with a finite rate k_2. The observed exchange rate (k_{ex}) is related to the kinetic parameters of this model according to the expression:

$$k_{ex} = k_1 k_2/(k_{-1}+k_2). \qquad (2)$$

It is useful to distinguish between two limits. If $k_2 \gg k_{-1}$ (EX_1 limit), then the observed exchange rate is governed by k_1:

$$k_{ex} = k_1. \qquad (3)$$

On the other hand, if $k_{-1} \gg k_2$ (EX_2 limit), then the exchange rate depends on k_2 as well as the steady-state populations of N and I:

$$k_{ex} = (k_1/k_{-1})k_2. \qquad (4)$$

In this case, k_2 limits the observed exchange rate, and the protein conformational states N and I equilibrate prior to the exchange event. Exchange rates for imidazole NH protons are pH-dependent (Wüthrich & Wagner, 1979) and, in general (Woodward *et al.*, 1982):

$$k_2 = k_A[\mathrm{H}^+]^m + k_B[\mathrm{OH}^-]^n + k_w, \qquad (5)$$

where the contribution from bulk water (k_w) is usually negligible. The magnitudes of k_A and k_B depend upon the local environment of the exchanging site. In the extreme where the exchange site is fully exposed to bulk water in state I (local unfolding model), k_A and k_B are expected to approach the values observed for model compounds. Alternatively, the local environment of state I may differ from that of bulk water (solvent penetration model), resulting in values of k_A and k_B that deviate from the corresponding values for model compounds and values for the exponents m and n, which may differ from unity.

The exchange rates for the distal histidine NH protons (Fig. 6) exhibit a pH dependence that is readily described by equation (5), suggesting that the EX_2 limit is applicable. Since there is, *a priori*, no reason to expect a pH dependence for the conformational equilibrium between N and I (there is no evidence for n.m.r. or electronic absorption spectroscopy for major changes with pH), we shall assume k_1/k_{-1} to be independent of pH. Thus, changes in k_1/k_{-1} due to effects other than pH scale the magnitude of the exchange rates at all pH values, but do not alter the position of the minimum of k_{ex} with respect to pH. Both wild-type and D60E exhibit a minimum in the exchange rate at approximately pH 9·2. The pH minimum for K45R, on the other hand, is approximately pH 9·8. This is consistent with a substantial reduction in the base-catalyzed exchange term $k_B[OH^-]^n$ for K45R with respect to wild-type. It is not surprising that k_2 should differ between wild-type and K45R, particularly in view of the large difference in the pH at which the minimum exchange rate occurs for the distal histidine NH proton relative to free imidazole, which has an exchange minimum below pH 5. It is then reasonable to suggest that the reduced exchange rate for the distal histidine NH of K45R results from an increased protection of this proton to base catalysis (lower k_B) in the I state. Alternatively, this difference could be associated with a decrease in the exponent n corresponding to a lower activity for OH^- at the exchange site. The reduction in the acid-catalyzed exchange rates for K45R relative to wild-type can be interpreted as the result of a decrease in k_a or a decrease in k_1/k_{-1}.

(b) *CO binding kinetics*

The rate of CO binding to Mb at room temperature has been observed to be more than an order of magnitude slower than the rates for O_2 and NO. The difference is considered to occur primarily in the bond-forming reaction at the heme iron, which is considered to be the dominant barrier for CO, whereas migration through the protein is considered to be rate-determining for O_2 and NO (Szabo, 1978; Olson *et al.*, 1987). This hypothesis is consistent with the observation that both the geminate yield and the rate of geminate recombination are markedly lower for CO (Henry *et al.*, 1983) than for O_2 or NO (Gibson *et al.*, 1986; Jongeward *et al.*, 1988). In order to provide a framework for discussion of our results, we invoke a scheme used by Henry *et al.* (1983) in their analysis of the room temperature recombination of CO to sperm whale Mb and by Murray *et al.* (1988) to analyze CO rebinding to a hybrid hemoglobin ($\alpha(Fe\text{-}CO)_2\beta(Co)_2$):

$$\underset{1}{Mb-CO} \underset{k_{21}}{\overset{k_{12}}{\rightleftharpoons}} \underset{2}{Mb:CO} \underset{k_{32}}{\overset{k_{23}}{\rightleftharpoons}} \underset{3}{Mb+CO}, \qquad (6)$$

where Mb−CO is the bound state, Mb:CO is the geminate state formed after bond dissociation, and Mb+CO is the deoxy state. Assuming a steady-state population of the geminate state, the rate constants of this kinetic scheme can be related to the observed on and off-rates according to the expressions:

$$k_{on} = k_{32}\phi_{gem} \qquad k_{off} = k_{12}(1-\phi_{gem}), \qquad (7)$$

where $\phi_{gem} = k_{21}/(k_{21}+k_{23})$ is the geminate recombination yield.

It is not possible to derive independent values for the kinetic constants associated with this scheme for our mutants, because we have only three observables, k_{on}, k_{off} and the relative geminate recombination yield. It is still instructive, however, to distinguish the two extreme cases in which the observed changes are associated entirely with the barrier at the heme iron (case I) or entirely with the barrier governing diffusion through the protein matrix (case II). This distinction is illustrated by Figure 7, where the potential energy of the system is considered as a function of the reaction co-ordinate. In case I, the mutation affects only k_{12} and k_{21}. Thus, the increase in k_{on} results directly from a 1·8-fold increase in ϕ_{gem} in accordance with equation (7). In case II, on the other hand, only k_{23} and k_{32} vary. Consequently, equation (7) predicts an increase in ϕ_{gem} of 2·5-fold or greater, given an upper limit of $\phi_{gem} = 0{\cdot}15$, which we estimate for wild-type. Our measurements of the geminate yields relative to sperm whale Mb indicate that the increase in ϕ_{gem} for K45R is less than a factor of 1·5 over that for wild-type, suggesting that neither of these cases adequately describes the effects of the mutation. We conclude, therefore that the mutation of lysine to arginine at position 45 affects both the inner as well as the outer barrier. Further analysis awaits more precise measurement of ϕ_{gem} and the kinetics of the geminate recombination process, which are in progress.

As mentioned earlier, the mutation of lysine 45 to

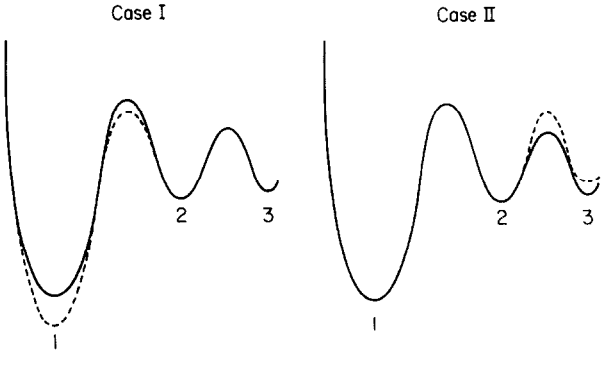

Figure 7. Schematic potential surfaces illustrating the possible consequences of the mutation at position 45. The curves represent relative potential energies of the wild-type (continuous lines) and K45R (broken lines), and have been superimposed so as to clearly indicate the association of the changes with the barrier at the heme iron (case I) or the barrier governing diffusion through the protein (case II). States 1, 2 and 3 refer to the bound, geminate and deoxy states, respectively.

arginine constitutes a conservative change on the surface of human Mb which is near, but not directly in the heme pocket. We initially expected that such a change might perturb the diffusion of ligands through the protein matrix but leave the barrier at the heme iron as well as the binding constant unaffected. It is surprising, therefore, to find that the barrier at the heme iron and the binding constant for CO have been perturbed. Preliminary results on the geminate recombination of NO on a picosecond time-scale, a process that is sensitive only to barriers near the heme iron, likewise demonstrate an effect of this substitution (Petrich & Martin, unpublished results).

In conclusion, we have shown that replacement of lysine 45 with arginine in human Mb influences both the on and off-rates for CO binding. In addition, the exchange rate for the distal histidine NH proton in the met cyano form is substantially reduced by this substitution. The exchange rates for K45R as a function of pH are similar to those for sperm whale Mb, which also has arginine at position 45, while wild-type human Mb follows the behavior of the horse and dog proteins (Lecomte & La Mar, 1985). No such correlation is observed in the rates for CO binding, implying that other substitutions also contribute to the differences in ligand-binding properties of Mbs from various species. Various kinetic and structural models that have been put forward to analyze previous data have been applied to the present case. The analysis of ligand dynamics in terms of specific molecular models is an intrinsically difficult proposition because the observables are rarely the elementary rates that appear in the models. Nonetheless, the models considered in this paper provide a reasonable working hypothesis, and specific predictions are made that are subject to further tests by other types of experiments and mutants. Though small in absolute magnitude, the changes observed in the present work are substantial given the conservative nature of the mutations. While less conservative mutations may produce more dramatic changes, the effects are not likely to be simple perturbations with localized consequences and may have little bearing on the native function of the protein.

We thank Drs R. Varadarajan and R. A. Goldstein for helpful discussion, Mike Fulton for large-scale fermentation, and Pam Patek for synthesis of oligonucleotides. This work was supported in part by NIH GM-27738. The 500 MHz n.m.r. spectrometer was supported through NSF DMB-8515942 and NIH 1-51-RR-2733. S.G.B. is the recipient of a Presidential Young Investigator Award, and matching funds were obtained from the Monsanto Corporation.

References

Alpert, B., El Mohsni, S., Lindqvist, L. & Tfibel, F. (1979). *Chem. Phys. Letters*, **64**, 11–16.

Antonini, E. & Brunori, M. (1971). *Hemoglobin and Myoglobin and their Reactions with Ligands*, North-Holland Publishing Co., Amsterdam.

Austin, R. H., Beeson, K. W., Eisenstein, L., Frauenfelder, H. & Gunsalus, I. C. (1975). *Biochemistry*, **14**, 5355–5373.

Breece, D., Eisenstein, L., Frauenfelder, H., Good, D., Marden, M. C., Reinisch, L., Reynolds, A. H., Sorensen, L. B. & Yue, K. T. (1980). *Biochemistry*, **19**, 5147–5157.

Case, D. A. & Karplus, M. (1979). *J. Mol. Biol.* **132**, 344–368.

Cutnell, J. D., La Mar, G. N. & Kong, S. B. (1981). *J. Amer. Chem. Soc.* **103**, 3567–3572.

Dalvit, C. & Wright, P. E. (1987). *J. Mol. Biol.* **194**, 313–327.

Doster, W., Beece, D., Bowne, S. F., DiIorio, E. E., Eisenstein, L., Frauenfelder, H., Reinisch, L., Shyamsunder, E., Winterhalter, K. H. & Yue, K. T. (1982). *Biochemistry*, **21**, 4831–4839.

Duddell, D. A., Morris, R. J. & Richards, J. T. (1979). *J. C. S. Chem. Commun.*, 75–76.

Duddell, D. A., Morris, R. J., Muttucumaru, N. J. & Richards, J. T. (1980). *Photochem. Photobiol.* **31**, 479–484.

Emerson, D. S., Lecomte, J. T. J. & La Mar, G. N. (1988). *J. Amer. Chem. Soc.* **110**, 4176–4182.

Friedman, J. M. & Lyons, K. B. (1980). *Nature (London)*, **284**, 570–572.

Gibson, Q. H. (1956). *J. Physiol.* **136**, 112–122.

Gibson, Q. H. & Roughton, F. J. W. (1957). *Proc. Roy. Soc. ser. B*, **146**, 44–56.

Gibson, Q. H., Olson, J. S., McKinnie, R. E. & Rohlfs, R. J. (1986). *J. Biol. Chem.* **261**, 10228–10239.

Goss, D. J., La Gow, J. B. & Parkhurst, L. J. (1982). *Comp. Biochem. Physiol.* **71B**, 229–233.

Hasinoff, B. B. (1977). *Arch. Biochem. Biophys.* **183**, 176–188.

Hasinoff, B. B. (1981). *J. Phys. Chem.* **85**, 526–531.

Henry, E. R., Sommer, J. H., Hofrichter, J. & Eaton, W. A. (1983). *J. Mol. Biol.* **166**, 443–451.

Hvidt, A. & Nielsen, S. (1966). *Advan. Protein Chem.* **21**, 287–386.

Jongeward, K. A., Magde, D., Taube, D. J., Marsters, J. C., Traylor, T. G. & Sharma, V. S. (1988). *J. Amer. Chem. Soc.* **110**, 380–387.

Kendrew, J. C., Dickerson, R. E., Strandberg, B. E., Hart, R. G., Davies, D. R., Phillips, D. C. & Shore, V. C. (1980). *Nature (London)*, **185**, 422–427.

Krishna, N. R., Huang, D. H., Glickson, J. D., Rowan, R. & Walter, R. (1979). *Biophys. J.* **26**, 345–366.

Kunkel, T. A. (1985). *Proc. Nat. Acad. Sci., U.S.A.* **82**, 488–492.

Kuriyan, J., Wilz, S., Karplus, M. & Petsko, G. A. (1986). *J. Mol. Biol.* **192**, 133–154.

La Mar, G. N. (1979). *Biological Applications of Magnetic Resonance* (Shulman, R. G., ed.), pp. 305–343, Academic Press, New York.

La Mar, G. N. & Krishnamoorthi, R. (1983). *Biophys. J.* **44**, 177–183.

La Mar, G. N., Budd, D. L. & Smith, K. M. (1980). *Biochim. Biophys. Acta*, **622**, 210–218.

Lecomte, J. T. J. & La Mar, G. N. (1985). *Biochemistry*, **24**, 7388–7395.

Levy, G. & Peat, I. (1975). *J. Magn. Reson.* **18**, 500–521.

Mabbutt, B. C. & Wright, P. E. (1985). *Biochim. Biophys. Acta*, **832**, 175–185.

Mayer, A., Ogawa, S., Shulman, R. G., Yamane, T., Cavaleiro, J. A. S., Rocha-Gonsalves, A. M. d'A., Kenner, G. W. & Smith, K. M. (1974). *J. Mol. Biol.* **86**, 749–756.

Murray, L. P., Hofrichter, J., Henry, E. R., Ikeda-Saito,

M., Kitagishi, K., Yonetani, T. & Eaton, W. A. (1988). *Proc. Nat. Acad. Sci., U.S.A.* **85**, 2151–2155.
Nobbs, C. L. (1966). In *Hemes and Hemoproteins* (Chance, B. Eastbrook, R. W. & Yonetani, T., eds), pp. 143–147, Academic Press, New York.
Olson, J. S., Rohlfs, R. J. & Gibson, Q. H. (1987). *J. Biol. Chem.* **262**, 12930–12938.
Perutz, M. F. & Matthews, F. S. (1966). *J. Mol. Biol.* **21**, 199–202.
Pitner, T. P., Glickson, J. D., Dadok, J. & Marshall, G. R. (1984). *Nature (London)*, **250**, 582–584.
Ringe, D., Petsko, G. A. Kerr, D. E. & Ortiz de Montellano, P. R. (1984). *Biochemistry*, **23**, 2–4.
Roder, H., Wagner, G. & Wüthrich, K. (1985). *Biochemistry*, **24**, 7396–7407.
Scouloudi, H. & Baker, E. N. (1978). *J. Mol. Biol.* **126**, 637–660.
Seidell, D. (1940). *Solubilities*, vol. 1, Van Nostrand, New York.
Sheard, B., Yumane, T. & Shulman, R. G. (1970). *J. Mol. Biol.* **53**, 35–48.
Springer, B. A. & Sligar, S. G. (1987). *Proc. Nat. Acad. Sci., U.S.A.* **84**, 8961–8965.
Szabo, A. (1978). *Proc. Nat. Acad. Sci., U.S.A.* **75**, 2108–2111.
Takano, T. (1977*a*). *J. Mol. Biol.* **110**, 537–568.
Takano, T. (1977*b*). *J. Mol. Biol.* **110**, 569–584.
Varadarajan, R. (1988). Ph.D. thesis, Stanford University, CA.
Varadarajan, R., Szabo, A. & Boxer, S. G. (1985). *Proc. Nat. Acad. Sci., U.S.A.* **82**, 5681–5684.
Varadarajan, R., Lambright, D. G. & Boxer, S. G. (1988). *Biochemistry*, in the press.
Waelder, S. F. & Redfield, A. G. (1977). *Biopolymers*, **16**, 623–629.
Waelder, S. F., Lee, L. & Redfield, A. G. (1975). *J. Amer. Chem. Soc.* **97**, 2927–2928.
Wang, C. & Pardi, A. (1987). *J. Magn. Reson.* **71**, 154–158.
Wiesenburg, D. A. & Guinasso, N. L. (1979). *J. Chem. Eng. Data*, **24**, 356–360.
Wittenberg, J. B., Wittenberg, B. A., Gibson, Q. H., Trinick, M. J. & Appleby, C. A. (1986). *J. Biol. Chem.* **261**, 13624–13621.
Woodward, C. K. & Hilton, B. D. (1979). *Annu. Rev. Biophys. Bioeng.* **8**, 99–127.
Woodward, C., Simon, E. & Tuchsen, E. (1982). *Mol. Cell. Biochem.* **48**, 135–160.
Wüthrich, K. & Wagner, G. (1979). *J. Mol. Biol.* **130**, 1–18.
Zoller, M. J. & Smith, M. (1983). *Methods Enzymol.* **100**, 468–500.

Edited by W. A. Hendrickson